

Copyright
by
Esmeralda Martinez
2018

**The Thesis Committee for Esmeralda Martinez Certifies that this is the approved
version of the following thesis:**

**Characterizing interactions between cAMP responsive element binding
protein 1 and methyl-CpG-binding protein 2 as a potential
transcriptional activation complex**

Committee:

Junji Iwahara, PhD, Mentor, Chair

Andrew Routh, PhD

Thomas Smith, PhD

Dean, Graduate School

**Characterizing interactions between cAMP responsive element binding
protein 1 and methyl-CpG-binding protein 2 as a potential
transcriptional activation complex**

by

Esmeralda Martinez, B.S.

Thesis

Presented to the Faculty of the Graduate School of

The University of Texas Medical Branch

in Partial Fulfillment

of the Requirements

for the Degree of

Master of Science

The University of Texas Medical Branch

August 2018

Para mi abuelito, Luciano López Banda, y mis padres, Adrián y María Martínez, quienes lucharon por las oportunidades que cosecho hoy como estadounidense.

Acknowledgements

I would like to thank my mentor, Dr. Junji Iwahara for all his guidance and assistance. I have gained independence, knowledge, and most importantly, work ethic and discipline to become a better scientist and professional in academia.

I would like to thank my committee members, Dr. Andrew Routh and Dr. Thomas Smith for their support and time. Collaborating with Dr. Routh to isolate nucleosomes and working in Dr. Smith's lab during my rotation were both essential experiences to understanding much of my biochemical work. I would also like to thank Dr. James Lee, who always instilled me with a mindset to think deeper and be more critical of science.

I would like to thank my lab members Dr. Catherine Kemme, Dr. Dan Nguyen and Ross Luu, for teaching me techniques, providing insight, and most importantly, being good friends when times were tough.

I would especially like to thank my best friend, Evelyn Valdez-Ward, who has always been supportive, empathetic, and listened to me during stressful times.

Finally, I would also like to thank my parents Adrian and Maria Martinez, who have always been my driving force to pursue my education and have supported me unconditionally throughout all my educational endeavors.

Characterizing interactions between cAMP responsive element binding protein 1 and methyl-CpG-binding protein 2 as a potential transcriptional activation complex

Publication No. _____

Esmeralda Martinez, M.S.

The University of Texas Medical Branch, 2018

Supervisor: Junji Iwahara

Transcriptional activity is controlled by many types of DNA binding proteins. In addition to transcription factors that activate transcription by recruitment of RNA polymerase II, there are proteins like methyl-CpG-binding protein 2 (MeCP2). MeCP2 regulates transcription by binding to methylated DNA. MeCP2 is traditionally associated with being a transcriptional repressor by binding to methylated CpG dinucleotides and recruiting corepressors. Literature has shown that MeCP2 is also a transcriptional activator and has been proposed to bind directly to cAMP responsive element binding protein (CREB1) to facilitate this action. This hypothesis is under-studied biochemically, and this project aims to elucidate biochemical and biophysical information to further understand this potential interaction. In this project, we qualitatively study protein-protein interactions between MeCP2 and CREB1 in solution through native polyacrylamide gel electrophoresis. We also examine this hypothesis quantitatively by examining the effects of MeCP2 on CREB1 binding to DNA through fluorescence anisotropy assays. These

studies suggest that there is a potential interaction between MeCP2 and CREB1. In addition to examining the presence of interactions between MeCP2 and CREB1, we also make progress on establishing protocols for studying the effects of nucleosomes on transcription factor target search. In summary, we establish purification protocols for CREB1 and MeCP2, preparation protocols for nucleosome core particle reconstitution, and examine interactions between CREB1 and MeCP2 through quantitative and qualitative methods.

TABLE OF CONTENTS

List of Tables	ix
List of Figures	x
List of Abbreviations	xiv
Chapter 1: Introduction	15
1.1 Transcription factors	15
1.1.2 Factors affecting transcription factor target search.....	18
1.2 Methyl-CpG-Binding protein 2	21
1.3 Hypothetical Model	23
1.3.2 MeCP2 MBD domain facilitates Egr-1 target search	24
1.3.3 MeCP2/CREB1 Transcriptional Activation Model	26
1.3.4 Relevance to Rett Syndrome and Neuronal Dysregulation	27
Chapter 2: Establishing protein purification methods	29
2.1 MeCP2 preparation	29
2.1.2 MeCP2 MBD-ATH1 Protocol	29
2.1.3 Full length MeCP2 Protocol	31
2.1.4 Discussion	33
2.2 CREB1 preparation.....	33
2.2.2 Protocol	33
2.2.3 Discussion	36
2.3 DNA preparation.....	37
Chapter 3: Examining potential direct MeCP2/CREB1 interactions.....	39
3.1. Native PAGE analysis	39
3.1.2 Results.....	39
3.1.3 Discussion	40
3.2. Fluorescence Spectroscopy Assays	41
3.2.2 Results.....	41
3.2.3 Discussion	43

Chapter 4: Towards the biophysical characterization of nucleosomal DNA in the target search process	45
4.1 Nucleosome Preparation	45
4.1.2 Nucleosome Core Particle Reconstitution	45
4.1.3 Chicken nucleosome purification	47
Chapter 5: Conclusions and future perspectives	50
5.1 MeCP2 and CREB1	50
5.2 Nucleosomal DNA in target search	52
Bibliography	53
Vita	63

List of Tables

Table 1:	Dissociation constants determined from fluorescence anisotropy binding assays.	43
----------	---	----

List of Figures

Figure 1:	Cis-regulatory elements of genes are controlled by trans-acting transcription factor proteins to either increase or decrease probability of initiating transcription.....	15
Figure 2:	Egr-1 and CREB1 DNA binding domains complexed with DNA crystal structures. Egr-1 has three zinc fingers, that each recognize three base pairs, connected by flexible linker DNA. CREB1 is a leucine zipper domain protein, with a homodimer formed through a dimerization interface.	16
Figure 3:	Transcription factors use several mechanisms for efficient target search within the genome.....	17
Figure 4:	Transcription factors like Egr-1 can become trapped at Natural Decoy sites that vastly outnumber functional target sites. “m” is the number of base pairs in a decoy sequence that match the recognition sequence. ...	19
Figure 5:	CpG dinucleotide methylation occurs symmetrically at the 5 position on the cytosine base. CpG Island methylation is rare while genomic methylation is common as shown on the chromosome.	20
Figure 6:	MeCP2 domains and crystal structure of MeCP2 MBD bound to methylated BDNF promoter DNA.....	21

Figure 7: Our hypothetical model of indirect transcriptional activation. MeCP2 is masking natural decoy (ND) sites to indirectly facilitate transcriptional activation by preventing transcription factors from becoming trapped.24

Figure 8: Schematic of experiments to test hypothetical model using stopped flow fluorescence assays.25

Figure 9: MeCP2 MBD-ATH1 purification protocol. Left panel: SDS-PAGE demonstrating pure protein. Right panel: workflow of MeCP2 MBD-ATH1 purification process.....29

Figure 10: Full length MeCP2 purification protocol. Left panel: SDS-PAGE demonstrating purified protein stored in solution and stored in lyophilized form. Right panel: workflow of full length MeCP2 purification process.....31

Figure 11: Established CREB1 purification. Left panel: SDS-PAGE demonstrating thioredoxin-CREB1 fusion protein denatured at 6 M urea from inclusion bodies, diluted using a refolding buffer containing arginine to facilitate refolding, CREB1 post cleavage using HRV-3C protease, and isolated CREB1 eluted in flow-through after Ni-NTA purification. Right panel: workflow diagram demonstrating overall purification steps for CREB1.34

Figure 12: Native PAGE analysis. Left: gel demonstrating increasing amounts of full length MeCP2 to CREB1. Right: gel demonstrating increasing amount of MeCP2 to CREB1.40

Figure 13: Fluorescence based protein titration assays. A) Full length MeCP2 titration to 10 nM FAMCRE33 probe. B) Full length MeCP2 titration to other nonspecific 10 nM FAM 33bp probe. C) CREB1 titration to 10 nM FAM33CRE probe before reducing treatment. D) CREB1 titration to 10 nM FAM33CRE probe after reducing treatment. E) CREB1 titration to 10 nM FAM33CRE probe in presence of 200 nM full length MeCP2. F) CREB1 titration to 10 nM FAM33CRE probe in presence of 30 nM full length MeCP2.43

Figure 14: Nucleosomal DNA preparation. Left panel: Native TBE polyacrylamide gel demonstrating confirmation of crDNA, FAM labeled W601 DNA, and reconstitution of nucleosome core particle. Right panel: Native TBE polyacrylamide gel demonstrating presence of genomic chicken DNA after purification from chicken blood. SDS-PAGE demonstrating presence of histone octamer after purification from chicken blood.49

List of Abbreviations

DNA	deoxyribonucleic acid
cAMP	Cyclic adenosine monophosphate
CREB1	cAMP responsive element binding protein 1
CV	Column Volumes
TF	Transcription factor
MeCP2	Methyl CpG binding protein 2
ND	Natural Decoy
FAM	fluorescein amidite

Chapter 1: Introduction

1.1 TRANSCRIPTION FACTORS

The haploid human genome is three billion base pairs. This vast amount of information is highly regulated. At the molecular level, genetic information is controlled in order to express certain genes in specific cell types. Although there are many steps in gene expression that can be regulated, transcriptional control guarantees that only specific gene targets are transcribed.¹ In the cell, proteins called transcription factors recognize specific regions of DNA to control genes. These regions of DNA are called cis-regulatory elements and are near genes (Figure 1). They contain specific sequences that transcription factors bind to in order to begin the cascade that leads to the recruitment of RNA polymerase II.¹⁻²

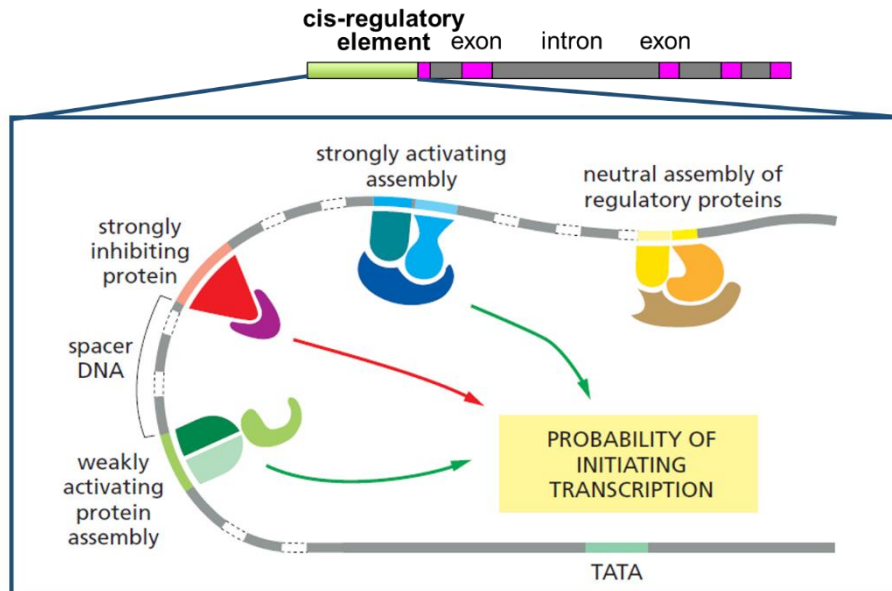


Figure 1: Cis-regulatory elements of genes are controlled by trans-acting transcription factor proteins to either increase or decrease probability of initiating transcription.

Transcription factors have high specificity for either a certain DNA structure³ or sequence⁴. Most transcription factor sequence recognition sites are relatively short sequences. The early growth response 1 (Egr-1) protein recognizes the nine base pair sequence, GCGTGGGCG. Egr-1 contains three zinc fingers in its DNA binding domain, where each zinc finger recognizes three base pairs of the target sequence, as shown in the left panel of Figure 2.⁵ Our lab has used Egr-1 as a model system for research to study protein-DNA interactions extensively. Similarly, cAMP response element binding protein 1 (CREB1) binds to the eight base pair sequence, TGACGTCA.^{6,7} CREB1 is a leucine zipper DNA binding domain protein, where a homodimer forms into a zipper like structure from two alpha helix monomers to form a short coiled coil. This zipper motif forks onto the major groove of DNA as shown in the right panel of Figure 2. CREB1 recognizes a palindromic sequence due to the homodimerization.⁸

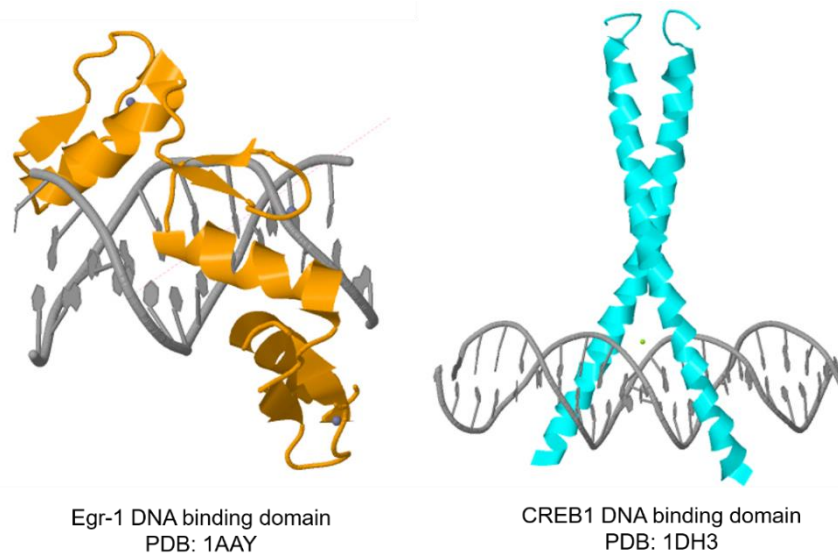


Figure 2: Egr-1 and CREB1 DNA binding domains complexed with DNA crystal structures. Egr-1 has three zinc fingers, that each recognize three base pairs, connected by flexible linker DNA. CREB1 is a leucine zipper domain protein, with a homodimer formed through a dimerization interface.

Although the concept of transcription factors finding their target sequence based on their own DNA binding motifs and structure may seem simple, the size of the human genome increases the complexity of transcription factors finding their target. Furthermore, transcription factors are not all produced constantly in the cell. Transcription factors are either constitutive or inducible. Constitutive transcription factors are always present in the cell, whereas inducible transcription factors need a stimulus to be produced. CREB1 is a constitutive transcription factor, and the activity in the cell is controlled by phosphorylation state.⁹ In contrast, Egr-1 is an inducible transcription factor, and is only produced in the cell when a visual or audible stimuli occur, and has a relatively short half-life of 0.5-1 hours after production. Once Egr-1 is produced, it is involved in learning, memory, and plasticity in the brain¹⁰

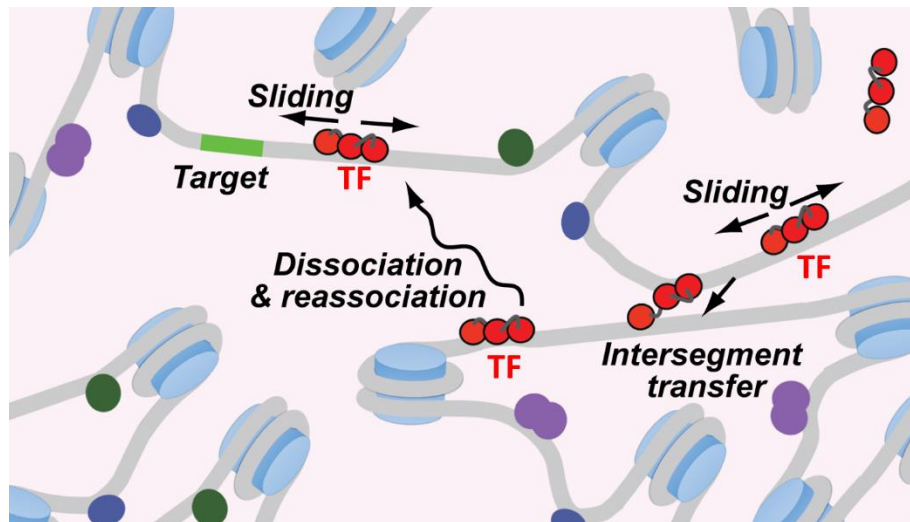


Figure 3: Transcription factors use several mechanisms for efficient target search within the genome.

How a transcription factor finds its target site in order for the cell to elicit a response in a timely manner is a problem that has been researched for decades. Through biophysical and biochemical work, literature has shown that there are several mechanisms transcription factors use to have efficient target search rates. Macroscopic dissociation and reassociation

is the process whereby proteins completely dissociate from DNA, and undergo Brownian motion to find a different segment of DNA on which to reassociate.¹¹ Secondly, proteins also undergo one-dimensional diffusion, where instead of undergoing random 3-dimensional Brownian motions within solution, they will bind nonspecifically to DNA and relocate without completely losing all interactions with DNA. This process is termed “sliding” and the efficiency is unique to every protein.¹² Finally, proteins can also undergo intersegment transfer.¹³ In this process, a protein will be bound to segment of DNA, and then simultaneously bind to another portion of DNA. The portions of DNA are typically not correlated, and this allows the protein to explore the genome (Figure 3). Collectively, these classical mechanisms allow proteins to efficiently search for their targets on DNA.

1.1.2 Factors affecting transcription factor target search

Natural Decoys (NDs)

Within the three billion base pairs of the haploid human genome, there are bound to be sequences that are similar or identical to known functional transcription factor target sequence sites. To calculate how many of these sites exist, our group has used a simple probabilistic calculation specific for 9-bp recognition sites ($n = 9$) as that of Egr-1, where the NDs exhibit a 7-bp match ($m = 7$). Specifically, the number of sites is determined by $2(1/4)^m(3/4)^{n-m}{}_n C_m$, which accounts for the matching and non-matching bases in the sequence. The factor of 2 is to account for the complementary sequence, and the ${}_n C_m$ is a mathematical combinatorial term.¹⁴ Overall, this gives a total of 10^7 estimated natural decoy sites for a transcription factor like Egr-1 in the haploid human genome. Although these sites may only differ by several base pairs, or be exactly the same sequence, when a transcription factor binds, there is no cascade of transcriptional events triggered, and are therefore nonfunctional. In addition, there are also sites within the genome that completely match the recognition target sequence, but simply have no function, or gene attributed to them.

We have previously demonstrated that these similar, high affinity sites can sequester transcription factors and cause them to become trapped.¹⁵ Subsequently, these endogenous, high affinity, quasi specific sites in the human genome can act as natural decoys (ND) to the transcription factor. NDs far exceed the number of functional target sites. If transcription factors are bound to these sites, they will not reach their target site and essentially become trapped (Figure 4). ND abundance and high affinity implicate them to be a major factor in transcription factor target search, and many questions about the implications remain to be addressed.

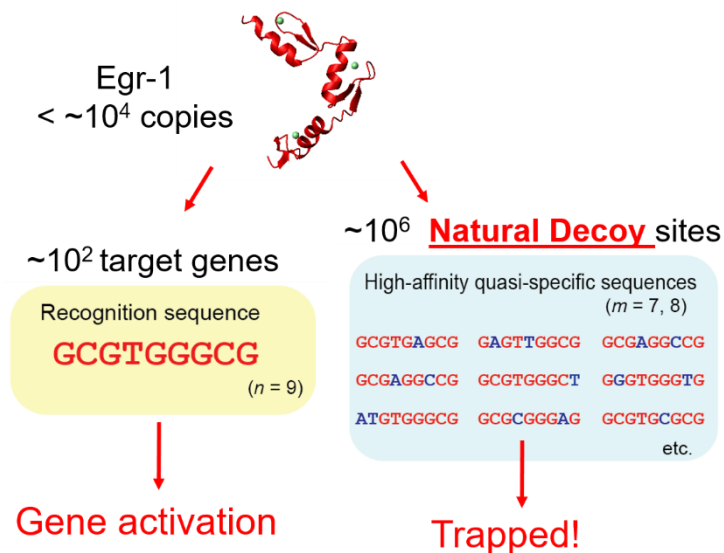


Figure 4: Transcription factors like Egr-1 can become trapped at Natural Decoy sites that vastly outnumber functional target sites. “m” is the number of base pairs in a decoy sequence that match the recognition sequence.

DNA methylation

DNA methylation is a covalent modification that occurs on cytosine bases, that allows for epigenetic changes but doesn't change DNA sequence.¹ In mammalian genomes, DNA methylation mostly occurs at CpG dinucleotides, where C is connected to a G base, and is base paired to the same sequence in the opposite direction on the complementary DNA strand.¹⁶ The CpG dinucleotide is methylated in this manner by the enzyme DNA

methyltransferase. DNA methylation is associated with silencing, where it can affect the binding of transcriptional regulators to DNA through steric interference.¹⁷

The overall density of CpG dinucleotides dispersed throughout the genome in most tissues is relatively low¹⁸, but there are regions of the genome that are CpG rich and are termed CpG Islands (CGI)¹⁷. CGIs range between 200 and 3000 base pairs in length,^{15, 19} are comprised of greater than 50% of G/C nucleotides, and are associated with over 70% of all gene promoters.^{17, 20, 21} The fact that so many genes are under control of promoters within CpG rich regions leads to the idea that methylation can control these genes. However, CGIs, including those associated with promoters, are rarely found to be methylated. In fact, although around 85% of the genome is methylated, only 6% of CGIs are methylated (Figure 5).²²

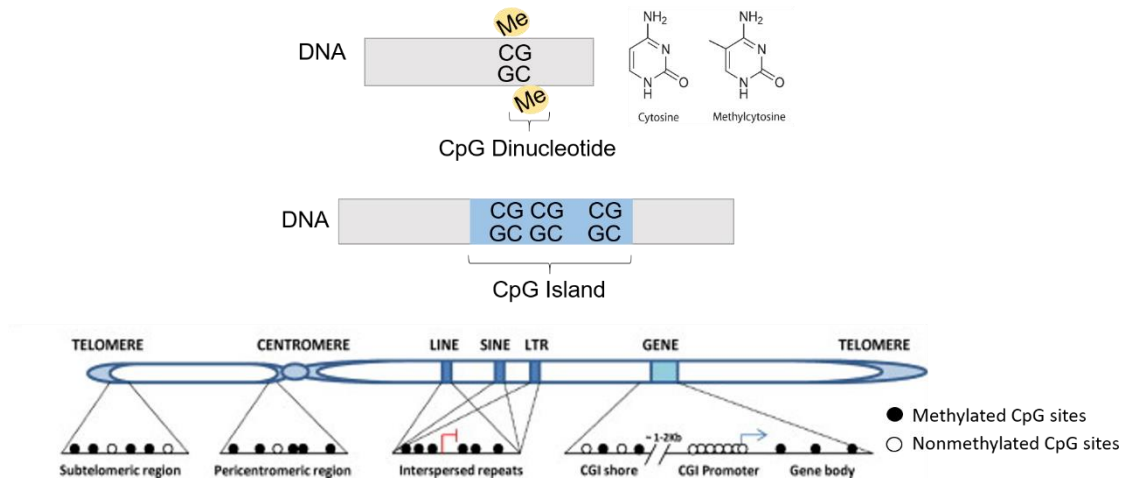


Figure 5: CpG dinucleotide methylation occurs symmetrically at the 5 position on the cytosine base. CpG Island methylation is rare while genomic methylation is common as shown on the chromosome.

1.2 METHYL-CPG-BINDING PROTEIN 2

MeCP2 Domains and Functions

Methyl-CpG-binding proteins, such as methyl-CpG-binding protein 2 (MeCP2), bind to methylated DNA and are typically associated with silencing through obstructing transcriptional activators from promoters and recruiting co-repressors via the transcriptional repressor domain.^{23, 24} MeCP2 is a 487 amino acid protein, composed of a Methyl-CpG dinucleotide binding domain (MBD), a transcriptional repression domain (TRD), and three AT Hook (ATH) regions.^{25, 26} MeCP2's MBD is ordered, forming a wedge like structure when bound to methylated DNA.²⁷ The other domains of MeCP2 have not been characterized extensively due to their intrinsic disorder.²⁸ The MBD has been crystallized when complexed with methylated DNA as shown in Figure 6,²⁹ but structural information and interactions between the other MeCP2 domains and DNA remains limited.

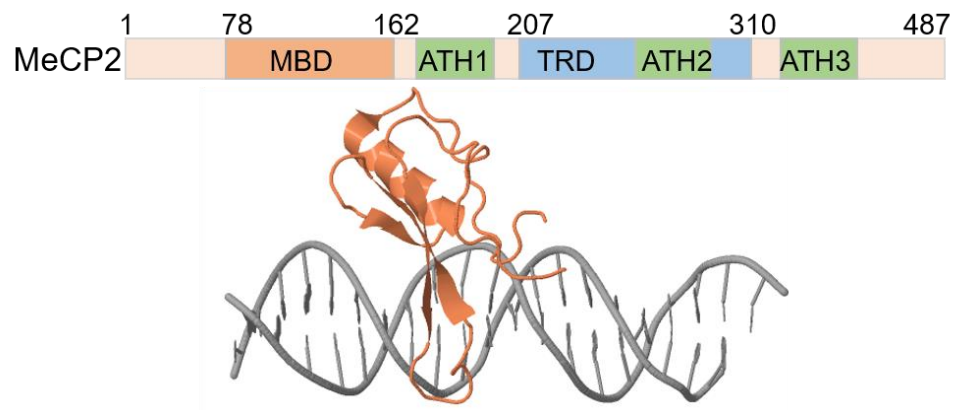


Figure 6: MeCP2 domains and crystal structure of MeCP2 MBD bound to methylated BDNF promoter DNA.

MeCP2 is a multifunctional protein and is ubiquitously expressed throughout human tissues, but expression is particularly high within the brain.³⁰ The expression levels

of MeCP2 in post mitotic neurons is near the levels of histone H1, making it an important transcriptional regulator.³¹ MeCP2 binds to methylated DNA through its core MBD domain, to a single, doubly methylated CpG dinucleotide.³² Association with a methylated CpG mediates transcriptional repression activity by facilitating the recruitment of corepressors like histone deacetylases and Sin3a.³² MeCP2 binds to these corepressors via the TRD and was shown to be responsible for MeCP2 mediated repression.

Evidence collected throughout the past several decades suggests that transcriptional repression is the primary function of MeCP2. Numerous recent studies have proposed novel functions of MeCP2 interacting with the genome, such as regulation of alternative splicing via an interaction with the transcription factor YB1, and regulation of microRNA processing by interfering with RNA splicing.³¹ Additionally, MeCP2 has also been proposed to bind to non-methylated DNA to compact chromatin.³³

MeCP2 has also been found to activate over 2000 genes³⁴ through gene knockout and overexpression studies in mice. These studies were pursued on the premise that MeCP2 loss and MeCP2 duplication both demonstrate neurological aberrations. Overexpression of MeCP2 was expected to cause more gene downregulation, based on the premise that MeCP2 is a transcriptional repressor. Knockout of MeCP2 was expected to cause more gene upregulation. Surprisingly, the results demonstrated that the overexpression of MeCP2 caused gene upregulation, and the opposite for MeCP2 knockout. These results suggested that MeCP2 also plays a regulatory role as a transcriptional activator.³⁴ This role in transcriptional activation is currently not well understood due to the lack of further biochemical studies. Through studying MeCP2 and its relationship with other transcription

factors³⁴, we will provide new insight on epigenetic regulation and its effects on neuronal processes.

1.3 HYPOTHETICAL MODEL

Many genes have transcription factor target sequences in CpG Islands (CGIs).³⁵ Approximately 70% of all gene promoters are associated with CGIs.^{20, 21} Consequently, many transcription factor target sequences are CpG rich. The Egr-1 and CREB1 target sequences are among many transcription factor recognition sequences that contain 1-2 CpG dinucleotides. However, there also exist many sequences in the genome that are similar to specific transcription factor target sequences, but are completely nonfunctional.¹⁵ Transcription factors can exhibit high affinity for these nonfunctional sequences, and may become trapped at these natural decoy sites (ND).³⁶ A vast majority of CpG dinucleotides are found outside of CGIs of the genome, and thus can be within the many potential ND sequences. Since ~85% of mammalian genome is methylated,³⁷ but most active gene promoters within CGIs are unmethylated,²² we can assume these CpGs within NDs are methylated. Surprisingly, only 0.8% of the human genome is comprised of CGIs, and they are rarely found to be methylated.³⁸ This conundrum would critically decrease the chance of MeCP2 suppressing transcription through binding to promoter sites in CGIs. Instead, there is a high chance of MeCP2 binding to methylated NDs.

Our hypothesis is that through binding to methylated natural decoys outside CGIs, MeCP2 indirectly guides some transcriptional activators to CGIs and thereby facilitates activation of genes downstream of CGI promoters. Based on our hypothesis, NDs outside of CGI promoter regions should be methylated, and MeCP2 should be bound to these regions. Since these CGIs inherently contain NDs, MeCP2 would be masking NDs and

facilitating target search for transcription factors. Since many NDs exist throughout the genome outside of CGIs, we can hypothesize that MeCP2 occupancy is higher at methylated CpG sequences in NDs. As shown in Figure 7, when MeCP2 is bound to these sites, thus masking them, it indirectly activates the target search for other transcription factors.

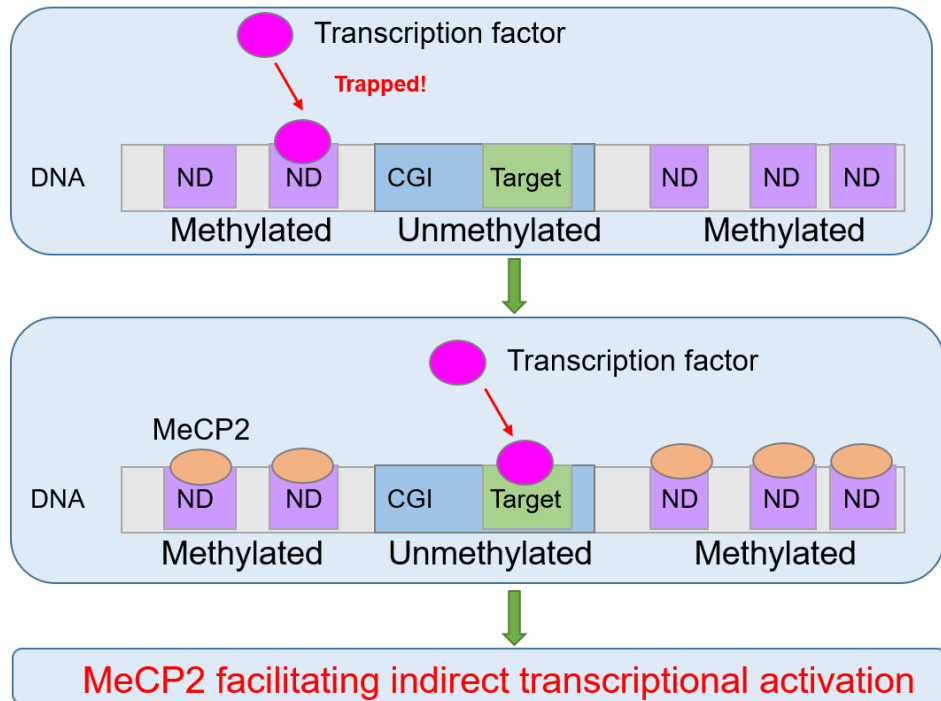


Figure 7: Our hypothetical model of indirect transcriptional activation. MeCP2 is masking natural decoy (ND) sites to indirectly facilitate transcriptional activation by preventing transcription factors from becoming trapped.

1.3.2 MeCP2 MBD domain facilitates Egr-1 target search

Our group has worked on testing this hypothesis through fluorescence spectroscopy assays. We conducted stopped flow fluorescence kinetic assays. These assays are performed by mixing a solution of protein and DNA to observe protein/DNA association through a decrease in fluorescence intensity. The DNA solution contains a fluorescently

tagged probe containing the protein target sequence and competitor DNA. When the two solutions are mixed, the protein binds to the target DNA to cause a decrease in fluorescence.³⁹

Using Egr-1 as a target search model system, we found that when the target sequence was methylated, association rate was not affected.⁴⁰ This information was critical in order to test our hypothetical model. If Egr-1 binding was affected by methylation, the effects of MeCP2 potentially occupying methylated natural decoys could not be evaluated since target search would be affected by methylation status instead of the presence of MeCP2.

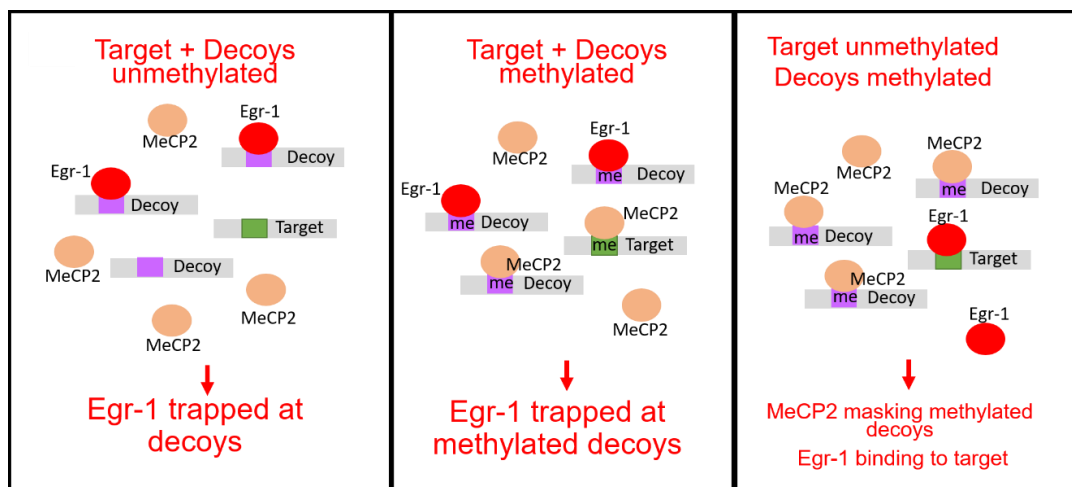


Figure 8: Schematic of experiments to test hypothetical model using stopped flow fluorescence assays.

Next, our group worked on evaluating the effect of MeCP2 on Egr-1 target search. We used DNA duplexes containing the target site, and duplexes containing natural decoys (NDs). In the presence of an unmethylated ND and MeCP2 (only the MBD domain), Egr-1 became trapped and the target search rate was much slower, as demonstrated in the left panel of Figure 8. In the presence of target site and decoy methylation and MeCP2, Egr-1 once again became trapped (center panel, Figure 8). Finally, in the presence of methylated decoy, unmethylated target site, and MeCP2, we observed a significant rescue in target search rate (Right panel, Figure 8). In this scenario, MeCP2 is bound to the methylated

decoys, while Egr-1 binds to the unmethylated target site. MeCP2 is masking the decoys in order for Egr-1 to find its target site.³⁶

1.3.3 MeCP2/CREB1 Transcriptional Activation Model

The current model proposed about MeCP2 transcriptional activation involves the transcription factor CREB1. Chahrour et al, suggests that MeCP2 is upregulating transcription by directly interacting with CREB1.³⁴ They suggest that MeCP2 will bind to methylated CpG site, and then recruit CREB1 to act as an activating complex. The authors propose the direct interaction model, but do not discuss potential interaction domains involved in the putative protein-protein interaction. Additionally, the genes they demonstrate that MeCP2 is upregulating are within CGIs that are not methylated. This model does not sufficiently answer the question of how MeCP2 is activating transcription. How is MeCP2/CREB1 complex upregulating so many targets that have unmethylated promoters, if the mediating interaction of the MeCP2/CREB1 complex to DNA is through MeCP2 binding to methylated DNA? Chahrour et al's findings support our proposed hypothetical model of indirect transcriptional activation by MeCP2 and transcription factors since the promoters of these genes are unmethylated. There is also a possibility that interactions between MeCP2 and CREB1 may decrease the amount of transcriptional repression MeCP2 can facilitate. We speculate that CREB1 may be interacting with MeCP2 by binding to the TRD. If CREB1 is interacting with this domain, it will prevent MeCP2 from recruiting corepressors and ultimately cause gene upregulation. Our work will elucidate information on the transcriptional activation that may be lost due to mutations in the MBD leading to reduced masking of NDs to facilitate TF target search, as well as the repressive activities that may be downregulated when CREB1 binds to the TRD. MeCP2 may act as a transcriptional activator through both modes, and this work will help us understand molecular level information about these complicated transcriptional regulation effects.

1.3.4 Relevance to Rett Syndrome and Neuronal Dysregulation

Rett syndrome (RTT) is one of the most prevalent causes of mental retardation in females, occurring in 1 out of 10,000 births worldwide.⁴¹ RTT is an X-linked dominant disorder, which causes lethality in hemizygous males⁴² and variable severity in females due to skewed X inactivation.⁴³ The classical clinical features of RTT includes slowed, regressing mental development early in life, accompanied with autistic behavior.⁴⁴ Several RTT clinical variants have been identified and studied for several decades, but a defined mechanism is still currently unknown.⁴⁵

Based on the neuronal global transcription activity loss when MeCP2 is deficient, its function as a transcriptional activator seems to be crucial for proper neuronal function.^{46,47} The specific mechanism for this wide gene activation is still unclear, since MeCP2 does not directly possess a transcriptional activation domain.⁴⁸ Indeed, clinical RTT variants display *MECP2* mutation hotspots in both the MBD and the TRD.^{49,50,25} This suggests that MeCP2's methylated DNA binding ability in RTT pathogenesis is as essential as its traditionally known function as a transcriptional silencer through its TRD.

DNA methylation at CpG dinucleotides in the brain has been shown to be a dynamic process that changes in response to lifestyle factors like sleep⁵¹, physical activity⁵², and even maternal care⁵³. Recent studies have indicated that the brain methylome changes in response to stimuli⁵⁴ and affects neuronal function such as synaptic plasticity⁵⁵ and memory formation.⁵⁶ However, any neuronal transcriptional activity effects caused by the dynamic brain methylome, remain to be addressed. Transcription factors implicated in activating memory response genes may show interplay with Methyl-CpG-binding proteins. This project will allow us to gain knowledge on how MeCP2's role as an indirect

transcriptional activator can affect neuron function in the context of RTT and epigenetic modifications.

Chapter 2: Establishing protein purification methods

2.1 MECP2 PREPARATION

2.1.2 MeCP2 MBD-ATH1 Protocol

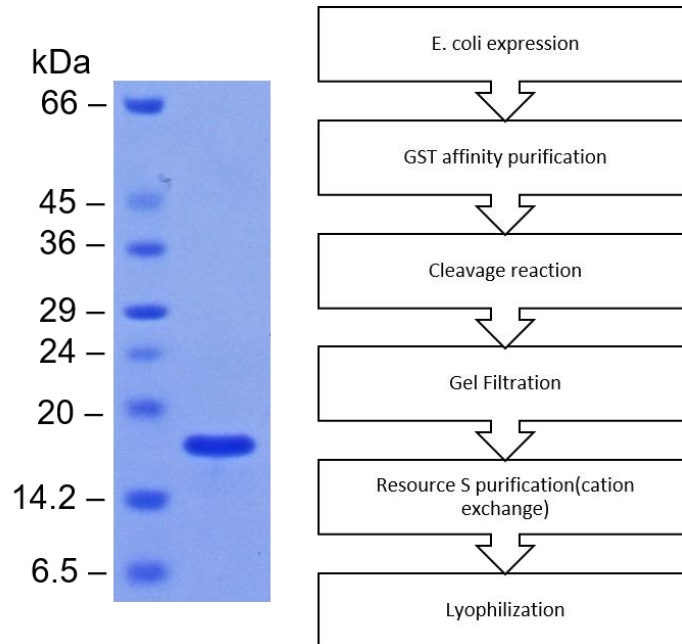


Figure 9: MeCP2 MBD-ATH1 purification protocol. Left panel: SDS-PAGE demonstrating pure protein. Right panel: workflow of MeCP2 MBD-ATH1 purification process.

The MeCP2-MBD-ATH1 construct consists of the methyl-CpG-binding domain (MBD) and the first AT-Hook of MeCP2. After several attempts to express a GST fusion MeCP2 protein, we found that overall expression and solubility were low. The MeCP2-MBD-ATH1 gene fused to a GST encoding gene was inserted into a pET49 plasmid with a kanamycin selection marker. This plasmid containing the protein fusion was transformed into *Escherichia coli* BL21(de3) bacterial competent cells and grown in a 4 liter culture containing minimal media enriched with isotopic ^{13}C glucose and ^{15}N ammonium chloride

to label the protein for NMR studies. The culture was grown at 37°C until the O.D.₆₀₀ reached ~1.0-1.2. Expression of GST-MeCP2-MBD-ATH1 was induced by 0.6 mM isopropyl B-D-1-thiogalactopyranoside, and the culture was grown at 37°C for 2 hours. The cells were harvested in a buffer containing 50 mM Tris-HCl, pH 7.5, 500 mM NaCl, 5% glycerol, 1% Triton X-100, and protease inhibitor tablets. The cells were sonicated using a Vibra-Cell Processor (Sonics) and then centrifuged at 4°C for 20 minutes at 20,000 rpm. The supernatant was collected and filtered through a 0.45 µm syringe filter. The protein was loaded onto a GSTPrep FF column (GE Healthcare) pre-equilibrated with buffer containing 50 mM Tris-HCl pH 7.5, 400 mM NaCl, 1% Triton X-100. The protein bound to the column was washed with the same buffer before being eluted with buffer containing 50 mM Tris-HCl pH 7.5, 400 mM NaCl, and 10 mM reduced glutathione. 100 U of HRV-3C protease (GE Healthcare) was added to the eluted protein, cleaved overnight at 4°C, and then concentrated to 10 mL using an Amicon Ultra centrifuge unit. The concentrated protein was loaded onto a Sephacryl S100 26/60 gel filtration column (GE Healthcare) equilibrated with buffer containing 50 mM Tris-HCl pH 7.5, 1 M NaCl, and 2 mM β-ME. The collected fractions containing protein were assayed by SDS-PAGE. The protein was loaded onto a Resource-S cation exchanged column (GE Healthcare) and eluted using a gradient from 200 mM NaCl – 1000 mM NaCl, and 50 mM Tris-HCl pH 7.0, 5% glycerol, and 1 mM β-ME. The protein was confirmed via SDS-PAGE (Figure 9) and then quantified using UV absorbance spectrum.

2.1.3 Full length MeCP2 Protocol

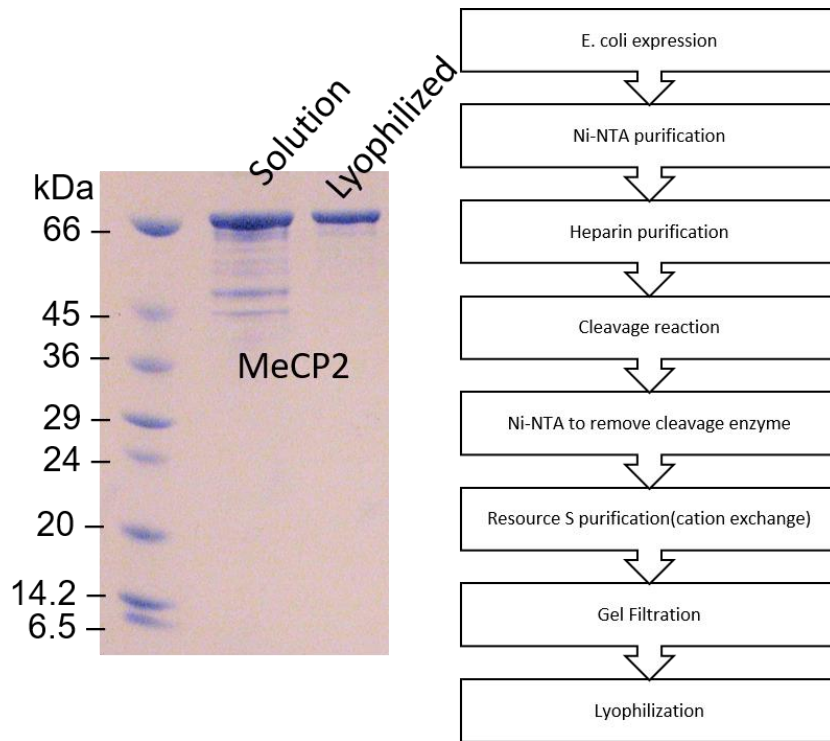


Figure 10: Full length MeCP2 purification protocol. Left panel: SDS-PAGE demonstrating purified protein stored in solution and stored in lyophilized form. Right panel: workflow of full length MeCP2 purification process.

The MeCP2 protein construct used in our lab previously consisted of only the methyl-CpG-binding domain (MBD) of MeCP2 (residues 335-423). In order to test interactions between MeCP2 and CREB1, we needed full length MeCP2. After several attempts to express a GST fusion MeCP2 protein, we found that overall expression and solubility were low. We sought out to use a different fusion tag and found that a thioredoxin (Trx) tag increased solubility and expression significantly.

The full length MeCP2 gene fused to a Trx encoding gene was amplified by PCR and inserted into a pET32a (+) plasmid with an ampicillin selection marker. This plasmid containing the protein fusion was transformed into *Escherichia coli* BL21(de3) bacterial competent cells and grown in a 4 liter culture containing minimal media enriched with

isotopic ^{13}C glucose and ^{15}N ammonium chloride to label the protein for NMR studies. The culture was grown at 37°C until the O.D._{600} reached ~ 0.8 . Expression of Trx-MeCP2 was induced by 0.4 mM isopropyl B-D-1-thiogalactopyranoside, and the culture was grown at 17°C overnight. The cells were harvested in a buffer containing 50 mM Tris-HCl, pH 7.5, 500 mM NaCl, 5% glycerol, 1% Triton X-100, and protease inhibitor tablets, after 18 hours of growth. The cells were sonicated using a Vibra-Cell Processor (Sonics) and then centrifuged at 4°C for 20 minutes at $20,000\text{ rpm}$. The supernatant was collected and filtered through a $0.45\text{ }\mu\text{m}$ syringe filter. The filtered lysate was loaded onto a nickel column connected to an ÄKTAfplc system, and equilibrated with a buffer containing 50 mM Tris-HCl pH 7.5, 100 mM NaCl, 20 mM Imidazole, 10% glycerol, 1 mM β -mercaptoethanol (β -ME). The column was washed with 10 CV of binding buffer, and then eluted using a gradient of 20 mM – 400 mM imidazole. Fractions containing UV absorbance peaks were assayed by SDS-PAGE, and were collected to load on a Heparin column also connected to an ÄKTAfplc system that was pre-equilibrated with a buffer containing 50 mM Tris-HCl pH 7.5 and 1 mM β -ME. The protein was eluted over a gradient from 0 - 1000 mM KCl. Fractions exhibiting UV absorbance at 280 nm were assayed by SDS-PAGE. The fusion protein was cleaved to remove the Trx tag using Human Rhinovirus 3C PreScission Protease (Genway) for four hours at 4°C . To remove the protease and cleaved Trx tag, the solution was loaded to a nickel column once again, using the same procedure. The cleaved protein was then loaded onto a Resource-S cation exchange column connected to an ÄKTAPurifier system, equilibrated with buffer containing 50 mM Tris-HCl, pH 7.5, 200 mM NaCl, 5% glycerol, and 1 mM β -ME. The protein was eluted over a gradient reaching 1 M NaCl. Finally, the protein was loaded onto a Sephacryl-200 size exclusion column equilibrated in buffer containing 0.2 M ammonium acetate, pH 7.0 and 1 mM β -ME. Fractions containing MeCP2 were pooled and purity was confirmed by SDS-PAGE (Figure 10). The purified MeCP2 solution was lyophilized and stored at 4°C .

2.1.4 Discussion

Before establishing this purification protocol for full length MeCP2, we attempted to express a GST fusion version. We found that expression was low, and most of the protein was in the pellet as inclusion bodies. To increase solubility of the expressed protein after induction, we decided to change the fusion tag to thioredoxin. Thioredoxin fusion tag has been demonstrated to increase solubility and prevent inclusion body formation.⁵⁷ The thioredoxin fusion tag contains a His tag, and MeCP2 coincidentally also contains an intrinsic His tag. This increased the number of purifications steps necessary because after cleavage of the Trx tag, it also bound to the Nickel column. We plan to remove the His tag fused to the Trx tag, to reduce the number of purification steps required. We also plan to store all protein through lyophilization after purification to prevent degradation.

2.2 CREB1 PREPARATION

2.2.2 Protocol

Transformation and culture

The full length Trx fusion CREB1 protein expression plasmid was transformed into *Escherichia coli* BL21(de3) competent cells. The cells successfully transformed with the plasmid containing ampicillin resistance and the CREB1 gene were selected for with 100 µg/ml ampicillin. These cells were then grown in a 4 liter LB media culture containing 100 µg/mL ampicillin and metal solution, at 37°C for 4 hours until the OD at 600 nm was ~0.8-0.9. At this point, protein expression was induced by 0.4 mM isopropyl B-D-1-thiogalactopyranoside, and cultivated for ~17 hours at 17°C. The cells were harvested by centrifuging at 4000 rpm, for 25 minutes at 4°C, and then resuspended with a buffer containing 50 mM Tris-HCl pH 7.5, 500 mM NaCl, 5% glycerol, 1% Triton X-100, and 3 protease inhibitor tablets. The cell suspensions were stored at -80°C until further use.

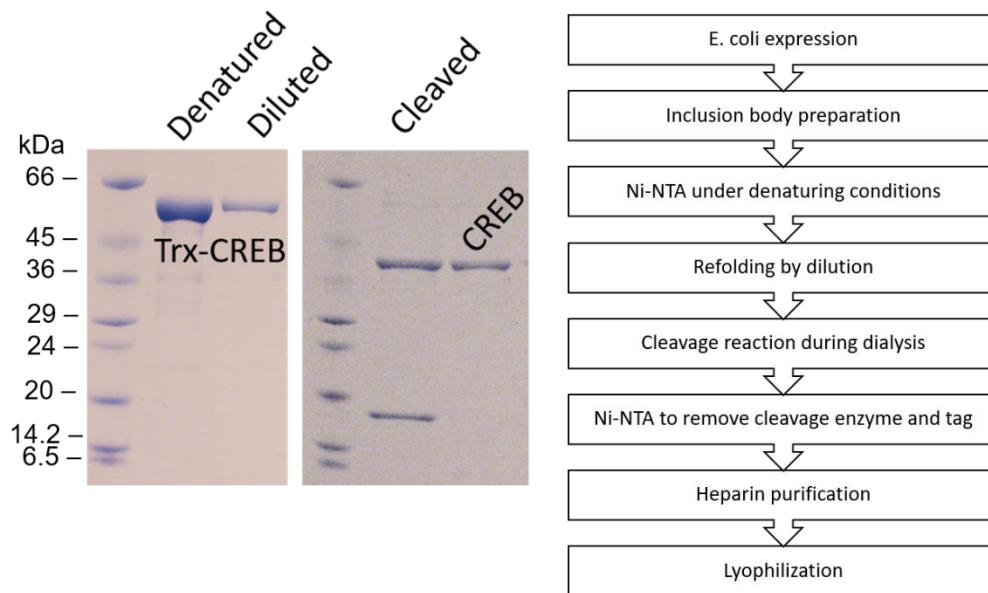


Figure 11: Established CREB1 purification. Left panel: SDS-PAGE demonstrating thioredoxin-CREB1 fusion protein denatured at 6 M urea from inclusion bodies, diluted using a refolding buffer containing arginine to facilitate refolding, CREB1 post cleavage using HRV-3C protease, and isolated CREB1 eluted in flow-through after Ni-NTA purification. Right panel: workflow diagram demonstrating overall purification steps for CREB1.

Extraction of inclusion bodies under denaturing conditions

The cells were thawed and sonicated at 4°C, using a 10 second on and 40 second off pulser setting, at 40% power, for 4 minutes total, using a Vibra-Cell Processor (Sonics). The Triton X-100 concentration was increased to 2% and incubated on ice for 10 minutes. The cells were centrifuged at 15000 rpm for 15 minutes at 4°C. The supernatant was discarded and the pellet was resuspended in buffer containing 50 mM Tris-HCl pH 7.9, 0.1 mM EDTA, 5% glycerol, 0.1 mM DTT, and 100 mM NaCl and 1% Triton X-100. The cells were centrifuged again and resuspended in the same buffer without Triton X-100.

Finally, the cells were centrifuged and resuspended in denaturing buffer containing 50 mM Tris-HCl pH 7.5, 6 M urea, 500 mM NaCl, 10% glycerol, and 1 mM β -ME. This cell suspension was rotated overnight at 4°C and centrifuged at 15000 rpm for 15 minutes at 4°C the following day. The supernatant was collected and filtered with 0.45 μ m syringe filters.

Ni-NTA under denaturing conditions

The filtered supernatant containing the denatured CREB1 protein was loaded onto a nickel column pre-equilibrated with buffer containing 50 mM Tris-HCl pH 7.5, 6 M urea, 500 mM NaCl, 5 mM Imidazole, 10% glycerol, and 1 mM β -ME. The protein was eluted using an imidazole gradient from 5 mM – 400 mM imidazole. The fractions demonstrating UV absorbance were collected after confirming presence of CREB1 through SDS PAGE. This solution was concentrated down to 5 mL using a 15 mL 10 kDa MWCO Amicon Ultra Centrifugal Unit.

Refolding by dilution

The denatured CREB1 was refolded through a 10x dilution using a buffer containing arginine that has been shown to facilitate folding of Trx tagged recombinant proteins.⁵⁸ The refolding dilution buffer contained 100 mM Tris-HCl pH 8.0, 0.7 M Arginine, 500 mM NaCl and 1 mM β -ME. The denatured, concentrated protein was diluted 10x, by adding 5 mL of protein dropwise into 45 mL of refolding buffer, while also swirling gently.

Cleavage during dialysis

The Trx tag on the fusion protein was cleaved through the addition of 100 units of Human Rhinovirus 3C PreScission protease (Genway) to the diluted protein. This cleavage

reaction solution was transferred to a dialysis membrane with a 3.5 kDa MWCO, in a reservoir buffer containing 20 mM Tris-HCl, pH 7.5, 500 mM NaCl, 10% glycerol, and 1 mM β -ME, and was dialyzed overnight at 4°C.

Ni-NTA under native conditions to remove Trx tag

The cleaved CREB1 solution was loaded onto a Ni-NTA column pre-equilibrated with 50 mM Tris-HCl pH 7.5, 500 mM NaCl, 5 mM Imidazole, 10% glycerol, and 1 mM β -ME. Since the (His)₆ tag was cleaved off with the Trx tag, the free CREB1 protein eluted in the flow through, as was confirmed by SDS-PAGE. The solution was concentrated using a VivaSpin 5 kDa MWCO centrifugal unit, down to 1 mL. The concentrated protein was diluted 5x with buffer containing 50 mM Tris-HCl pH 8.0, 1 mM MgCl₂, 2 mM DTT, and 20% glycerol and no salt to reduce the salt concentration to 100 mM NaCl.

Heparin column chromatography

To further remove nucleic acid contamination, the solution was loaded onto a Heparin cation exchange chromatography column, pre-equilibrated with buffer containing 50 mM Tris-HCl pH 8.0, 100 mM KCl, 1 mM MgCl₂, 2 mM DTT, and 20% glycerol. The protein was eluted over a gradient ranging from 100 mM KCl to 1 M KCl. Fractions containing protein confirmed by SDS-PAGE (Figure 11) were collected.

2.2.3 Discussion

Purifying this protein required extensive optimization since our lab did not have experience with refolding proteins from inclusion bodies. From establishing this protocol, we discovered several important aspects and steps necessary to refold CREB1 with high yield. Although this protein also has a Trx tag, solubility was not increased, and about 90% of the protein was expressed in inclusion bodies. We extracted using 6 M urea and found

that a triton treatment to remove membrane proteins was especially helpful. After extraction, we found that an initial Ni-NTA purification was essential in removing a considerable amount of the nucleic acid contamination. During refolding, we found that dilution with arginine was essential to significantly reduce precipitation. After refolding by dilution, the presence of glycerol increased yield by facilitating CREB1 stability and decreasing precipitation and aggregation. Finally, the most significant finding was that CREB1 is easily oxidized and is sensitive to temperature. We found that the presence of a reducing agent, 20 mM β -ME, at a relatively high concentration and low temperature was essential to keep the protein in solution.

2.3 DNA PREPARATION

The probe DNA duplex used in fluorescence experiments contained the CREB1 cAMP responsive element (CRE) binding sequence, TGACGTCA, three base pairs away from the 5'-end to which a fluorescein amidite (FAM) label is attached. The 33 base pair FAM labeled strand containing the CRE site, and a 33 base pair complementary strand, were purchased from Integrated DNA Technology (IDT). These DNA single strands were HPLC grade purified. These two single strands were annealed to form a dsDNA duplex and then purified on a Mono-Q anion exchange chromatography column connected to an ÅKTA Purifier system, that was pre-equilibrated with buffer containing 50 mM Tris-HCl pH 7.5, 1 mM ethylenediaminetetraacetic acid (ETDA). The dsDNA duplex was eluted over a gradient of 0 – 1.5 M NaCl. The fractions displaying UV absorbance at 260 nm were collected, concentrated with a 4 mL 3 kDa MWCO Amicon centrifugal unit. The UV absorbance spectrum was measured and, the 260 nm absorbance values were averaged. The extinction coefficient was estimated from the values provided by Integrated DNA

Technologies for the single DNA strands. Using the absorbance values measured and the estimated extinction coefficient, the protein concentration was quantified.

Chapter 3: Examining potential direct MeCP2/CREB1 interactions

3.1. NATIVE PAGE ANALYSIS

To begin qualitatively examining whether MeCP2 and CREB1 interact, we completed Native PAGE analyses. MeCP2 has a very basic pI, while CREB1 has an acidic pI. We hypothesized that if they do form a complex, we could potentially see this interaction on a Native PAGE, where charge would determine mobility and shift.⁵⁹ If they form a complex, the combined pI of the complex would change in comparison to each individual pI, and we could visually observe the potential complex as a shifted band.

3.1.2 Results

We qualitatively examined potential MeCP2/CREB1 interactions by running varying ratios of the protein mixtures on SurePAGE Bis-Tris 4-20% gradient gels. The samples were prepared by mixing with glycerol and normalizing volumes. The samples were loaded and electrophoresis was performed for 2-3 hours at 4°C. The results show that CREB1 migrates into the gel and demonstrates a relatively sharp band. As the amount of full length MeCP2 increases, the band begins to disappear by becoming fainter and less sharp. Another major difference is the “aggregate” that seems to form at the bottom of the well. As full length MeCP2 increases, the “aggregate” decreases as well. For MeCP2 MBD-ATH1, we do not see the same distinct disappearance of the CREB1 band, and aggregate. Instead, the band seems to migrate slightly slower, and there is still significant aggregate in the wells.

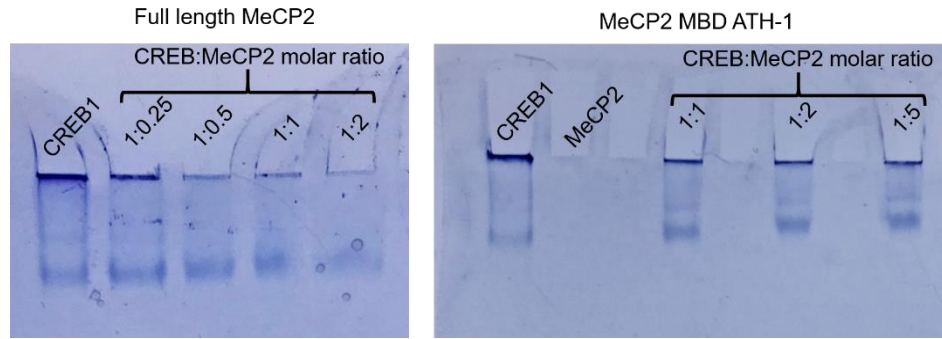


Figure 12: Native PAGE analysis. Left: gel demonstrating increasing amounts of full length MeCP2 to CREB1. Right: gel demonstrating increasing amount of MeCP2 to CREB1.

3.1.3 Discussion

These native gels were run using a normal current, which means that any negatively charged molecule will travel down into the gel. CREB1 is negatively charged, while MeCP2 is positively charged. When current is applied to these proteins in the gel, CREB1 should travel into the gel towards the positive current and MeCP2 should travel away and out of the gel. We also know that the MeCP2/CREB1 complex has a predicted pI of 9.58, based on ExPASy ProtParam calculation tool. Based on this information, if the proteins are complexing together, they should migrate up, away from the current, and out of the gel. Based on the results, as the amount of full length MeCP2 increases, the CREB1 band disappears, as shown in Figure 12. Qualitatively, the band of CREB1 becoming fainter is indicating that a complex is forming, and it is migrating away from the gel since it has a higher pI. Additionally, these results also seem to indicate that the ratio of the complex formation may be 1:1 since at 1:0.25 (CREB1:MeCP2), the amount of MeCP2 doesn't seem to change the band intensity, in comparison to when the ratio is 1:1. The volumes of solutions for the molar ratios used were calculated from the quantified protein concentrations. All protein concentrations were quantified by UV absorbance values, and estimated extinction coefficients from ExPASy.

We also tested the effect of MeCP2 MBD-ATH1 on CREB1 migration into the native gel (Right panel, Figure 12). As MeCP2 MBD-ATH1 increases, the band seems to shift upward, indicating a slower migration, but CREB1 still seems to aggregate in the bottom of the loading well. This may indicate that a complex isn't forming, or not as effectively as when full length MeCP2 is present. This information informs us on the potential domains involved in the protein-protein interactions between CREB1 and MeCP2. This may suggest that one of the domains not present in ATH1 such as the TRD, is facilitating the binding to CREB1. Additional extensive and quantitative studies are necessary to determine more details.

3.2. FLUORESCENCE SPECTROSCOPY ASSAYS

Protein binding can be quantitatively measured through fluorescence spectroscopy methods like the measurement of anisotropy. Fluorescence anisotropy is dependent on the presence of a fluorescent molecule, and the measurement of intensity and polarization of the emitted light by a fluorospectrophotometer. The fluorescent molecule is illuminated with polarized light at a certain wavelength that causes excitation. If the fluorescent molecule is free, and tumbling very fast in solution, the emitted light will be depolarized. Fluorescence anisotropy is the directional effect of the polarized light caused by the fluorescent molecule speed in solution. If the emitted light is depolarized, a low anisotropy value will be measured. When the fluorescent molecule binds to another molecule, it will tumble slower in solution. This slow tumbling will cause the emitted light to be polarized at the same angle it was excited at, which contributes to a high anisotropy value.¹

3.2.2 Results

To determine CREB1/MeCP2 interactions and affinities, we prepared a fluorescein amidite (FAM) labeled 33 base pair DNA probe that contained the CREB1 cAMP responsive element (CRE) consensus sequence. MeCP2 and CREB1 were prepared as

described in Chapter 2. Affinity measurements were determined using fluorescence anisotropy as a function of protein concentration (0.25-1200 nM). Fluorescence changes were measured using an ISS PC-1 Spectrofluorometer.

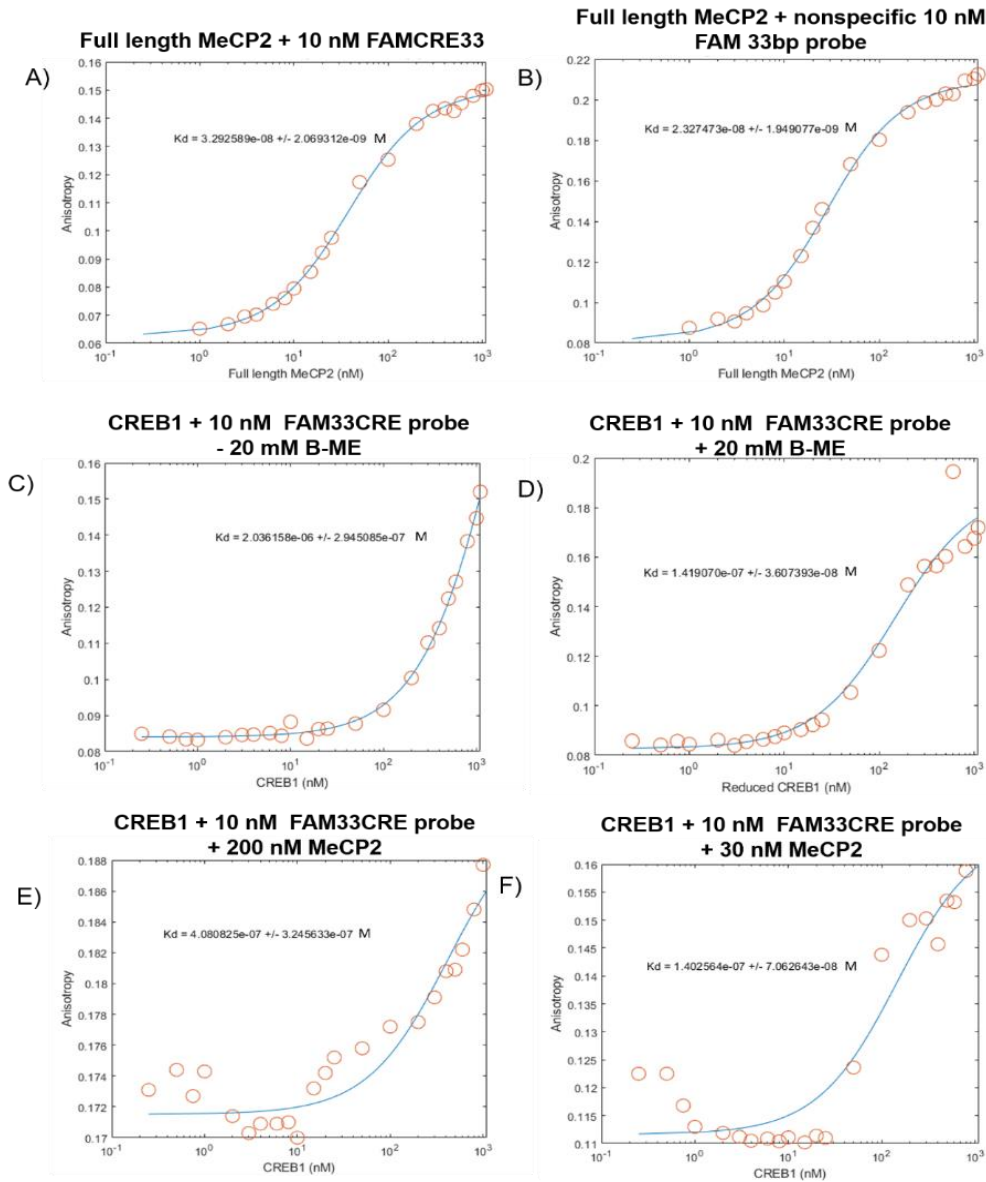


Figure 13: Fluorescence based protein titration assays. A) Full length MeCP2 titration to 10 nM FAMCRE33 probe. B) Full length MeCP2 titration to other nonspecific 10 nM FAM 33bp probe. C) CREB1 titration to 10 nM FAM33CRE probe before reducing treatment. D) CREB1 titration to 10 nM FAM33CRE probe after reducing treatment. E) CREB1 titration to 10 nM FAM33CRE probe in presence of 200 nM full length MeCP2. F) CREB1 titration to 10 nM FAM33CRE probe in presence of 30 nM full length MeCP2.

The assays were performed at 20°C in a buffer containing 50 mM Tris-HCl, pH 8.0, 100 mM KCl, 10 mM MgCl₂, and 20 mM β-ME. The dissociation constant was calculated from anisotropy data using a non-linear least-squares fitting using MatLab software as described in Zandarashvili et al,⁴⁰ and the curves are demonstrated in Figure 13.

	K_D
FL MeCP2 + 10 nM FAMCRE33	32 nM
FL MeCP2 + 10 nM FAM nonspecific 33	23 nM
Oxidized CREB1 + 10 nM FAM33CRE	2 uM
Reduced CREB1 + 10 nM FAM33CRE	141 nM
CREB1 + 10 nM FAM33CRE + 200 nM FL MeCP2	400 nM
CREB1 + 10 nM FAM33CRE + 30 nM FL MeCP2	140 nM

Table 1: Dissociation constants determined from fluorescence anisotropy binding assays.

3.2.3 Discussion

We discovered how sensitive CREB1 is to oxidation after initially observing a very weak affinity of 400 nM. Once we treated CREB1 with 20 mM β-ME, we saw a significant ~3x increase in affinity of around 140 nM. (Figures 12c and 12d) Next, we tested the affinity of MeCP2 to the CREB1 DNA probe, to determine what concentration to test the effect of MeCP2 presence on CREB1 binding. Our binding assays indicate that full length MeCP2 has a high affinity to nonspecific DNA (Figures 12a and 12b). Although it is

characterized to be a sequence specific binding protein through its MBD to methylated CpG dinucleotides, there have been numerous reports that show MeCP2's affinity for methylated DNA is only 3-fold higher than affinity for nonmethylated DNA.⁶⁰ We conducted these assays to determine a concentration at which we could test the effects of the presence of MeCP2 on CREB1 binding. After observing these high affinities, we decided to test a concentration of MeCP2 close to the affinity demonstrated in the binding assays (30 nM) and a higher concentration close to the affinity of CREB1 to its target site (200 nM). The results showed an increase in the initial anisotropy values. This increase was expected since anisotropy is directly affected by molecular size. If MeCP2 immediately associated with the probe DNA, it would decrease tumbling, and cause an increase in anisotropy. After observing the initial increase, we also saw a sudden decrease in anisotropy, which we speculate is CREB1 displacing MeCP2 on the DNA probe. Once this occurs, MeCP2 is free in solution and can potentially interact with CREB1. At 200 nM MeCP2, the affinity of CREB1 to the probe was ~3x weaker. At 30 nM, the affinity was almost the same as in the absence of MeCP2. (Figures 12e and 12f).

Overall, these results indicate that we have established a system we can use to further test how the presence of MeCP2 affects CREB1 binding. In the future, we can potentially optimize the assays by mixing CREB1 and MeCP2 in a 1:1 molar ratio, and allowing binding to occur, and then titrating this complex to DNA and observing anisotropy changes. We can also fluorescently tag the proteins and perform FRET experiments.

Chapter 4: Towards the biophysical characterization of nucleosomal DNA in the target search process

4.1 NUCLEOSOME PREPARATION

Nucleosomes have been shown to be dynamic in structure, where the DNA ends can unwrap from the histone octamer⁶¹ and DNA can become accessible to TFs. Considering how dynamic nucleosomes are, it is important to study the effect on transcription factor target search in nucleosomes to help us understand our hypothesis at the chromatin level. In order to test the effect nucleosomal DNA accessibility on TF target search at the chromatin level, we plan to use stopped-flow fluorescence kinetic assays. We will reconstitute mononucleosomes that contain target sequences of CREB1 and Egr-1 close to the DNA ends that are accessible for TF binding and assess effect on target search after mixing nucleosomes complexed with MeCP2 and either Egr-1 or CREB1. Overall, we have made significant progress on establishing protocols for preparing materials necessary for this branch of our research.

4.1.2 Nucleosome Core Particle Reconstitution

FAM-W601 Preparation

The DNA used to reconstitute the nucleosome core particle contained the Widom's 601 (W601) sequence, which is a well-positioned sequence that wraps around the histone octamer with high affinity.⁶² An HPLC purified 5' fluorescein amidite (FAM) labeled 37-mer single stranded DNA primer and an unlabeled reverse primer were purchased from Integrated DNA Technologies. These primers were used in PCR using the pGEM3Z/601 plasmid as a template, and Vent DNA Polymerase (New England Biolabs), in order to amplify a FAM labeled W601 DNA sequence. After PCR, the FAMW601 DNA product

was loaded to MonoQ anion exchange column pre-equilibrated with 50 mM Tris-HCl pH 7.5, and 1 mM EDTA. The FAMW601 was eluted using a gradient of 0 – 1.5 M NaCl. The fractions containing the FAMW601 were confirmed on a 1% agarose gel. The fractions were concentrated down to ~50 μ L, and then further purified by running on a TBE-PAGE 4-20% gel (Invitrogen). The portion of gel containing the DNA was excised, crushed and agitated at ambient temperature for 18 hours in buffer containing 10 mM Tris-HCl pH 7.5 and 40 mM KCl, in order to solubilize the DNA. Finally, the FAMW601 was purified with a PCR Purification Kit (Qiagen) and quantified using a UV absorbance spectrum.

crDNA prep

Nonspecific competitor DNA (crDNA) was prepared for the nucleosome particle reconstitution in order to saturate any histones that did not form an octamer. The crDNA was generated through polymerase chain reaction (PCR). Single stranded 27-mer and 28-mer forward and reverse DNA primers were ordered from Integrated DNA Technologies and we PCR-amplified the nonspecific crDNA using pUC-19 plasmid as a template and Vent DNA Polymerase (New England Biolabs). The PCR product was loaded to a Resource-Q anion exchange column pre-equilibrated with 50 mM Tris-HCl pH 7.5, and 1 mM EDTA. The crDNA was eluted using a gradient of 0 – 1.5 M NaCl. The fractions demonstrating UV 260 nm absorbance were concentrated down to ~500 μ L using an Amicon Ultra Centrifugal unit. The purified PCR product was then finally purified using a PCR Cleanup Kit (Qiagen) and quantified.

NCP reconstitution through dialysis to decrease salt concentration (NEB)

The nucleosome core particles (NCP) were formed through sequential dialysis over time to decrease salt concentration. The decreasing salt concentration drives nucleosome formation by allowing the negatively charged DNA to interact with the very basic histone octamer. After generating the competitor DNA and the FAM labeled W601 DNA, the EpiMark Nucleosome Assembly Kit (New England Biolabs (NEB) Inc.) was used to reconstitute unmodified recombinant human nucleosomes. Dialysis buffers containing 20

mM Tris-HCl, pH 8.0, 1 mM EDTA, 1 mM DTT, and decreasing amounts of NaCl (1.5 M NaCl, 1.0 M NaCl, 0.6 M NaCl, 0.25 M NaCl) were prepared and chilled to 4°C. The nucleosome reaction mixture was prepared following the NEB Dialysis Assembly Protocol (E5350) and transferred to a mini dialysis cassette unit. The reaction mixture was dialyzed against the 1.5 M NaCl buffer for 2-3 hours, and then transferred to the 1.0 M NaCl for 2-3 hours. The reaction was dialyzed against the 0.6 M NaCl buffer overnight, and then transferred to the 0.25 M NaCl the following day for at least 2-3 hours. All dialysis steps were at 4°C. The reaction mixture was removed from the dialysis cassette and transferred to a microcentrifuge tube, and stored at 4°C. The nucleosome formation was confirmed by running on a TBE-PAGE 4-20% gel (Invitrogen) comparing to the crDNA and W601. The NCP formation was confirmed through the shift of the free DNA band to a higher molecular weight at around 700 bp, demonstrated in Figure 14

4.1.3 Chicken nucleosome purification

In order to conduct stopped flow experiments using nucleosomal DNA, a larger quantity of histone octamers was required to reconstitute a larger yield of NCPs. Purifying histone octamers from chicken blood has been an established protocol for many years, and with the guidance of Dr. Andrew Routh's group, we purified soluble chromatin from chicken blood.

Chicken blood was purchased as a 25 mL aliquot bled into trisodium citrate. Upon arrival, the chicken blood was immediately added into 100 mL of Buffer-A (B-A) containing 60 mM KCl, 12 mM NaCl, 12 mM potassium cacodylate pH 6.0, 15 mM β -ME, 0.15 mM spermine, 0.5 mM spermidine, and 2 mM EDTA. The container in which the blood arrived was washed with an additional 50 mL of B-A and added to the diluted blood. The diluted blood was divided into 50 mL conical tubes and centrifuged at 4000 rpm for 8-10 minutes in order to pellet the blood cells. After carefully removing the supernatant, the pellet was washed with B-A twice more. The cells were then lysed with Buffer-B (B-

B), containing 60 mM KCl, 12 mM NaCl, 12 mM potassium cacodylate pH 6.0, 15 mM β -ME, 0.15 mM spermine, 0.5 mM spermidine, 2 mM EDTA, and 0.5% Triton X-100. In this buffer, the Triton X-100 nonionic surfactant lyses the cells by permeabilizing the blood cell membranes, and in turn releases the nuclei containing the chromatin. The nuclei were washed twice more with B-B. The nuclei pellet was then washed three times with Buffer-C (B-C), containing 60 mM KCl, 12 mM NaCl, 12 mM potassium cacodylate pH 6.0, 15 mM β -ME, 0.15 mM spermine, 0.5 mM spermidine, and 0.5% Triton X-100, until the pellet was colorless. The pellet was resuspended and washed two times in Buffer-D (B-D), containing 60 mM KCl, 12 mM NaCl, 10 mM Tris-HCl pH 8.0, 15 mM β -ME, 0.15 mM spermine, 0.5 mM spermidine, and 0.5% Triton X-100. After washing with B-D, the pH was high enough to begin digestion of the chromatin DNA using Micrococcal Nuclease (MNase). After conducting a trial digestion, the chromatin was incubated at 37°C, and 1 mM CaCl₂ was added. MNase was added to the solution and the chromatin was digested for 8 minutes. After eight minutes, the reaction was quenched by increasing the concentration of EDTA to 10% v/v. The nuclei containing the digested chromatin was lysed after centrifuging at 4000 rpm for 4 minutes, by resuspending in 20 mL Buffer-E, containing 10 mM Tris-HCl pH 7.4, and 0.2 mM EDTA. The nuclei were incubated on ice to allow for lysis to release the chromatin in solution. This soluble chromatin was centrifuged to pellet out the nuclear debris, and the supernatant containing the chromatin was transferred to a beaker. The salt concentration in the soluble chromatin was increased to 0.65 M NaCl using 5 M NaCl stock, in order to release linker Histones and HMG proteins.

The soluble chromatin was loaded onto a Sepharose 4B-Cl gel filtration column, pre-equilibrated with 0.65 M NaCl, 10 mM sodium cacodylate pH 6.0, and 0.2 mM EDTA. The flow-through was collected, and 1 column volume of buffer was run through the column (600 mL) to collect 7 mL elution fractions. The fractions demonstrating UV

absorbance were run on an SDS-PAGE to confirm presence of the histone octamer as shown in Figure 14.

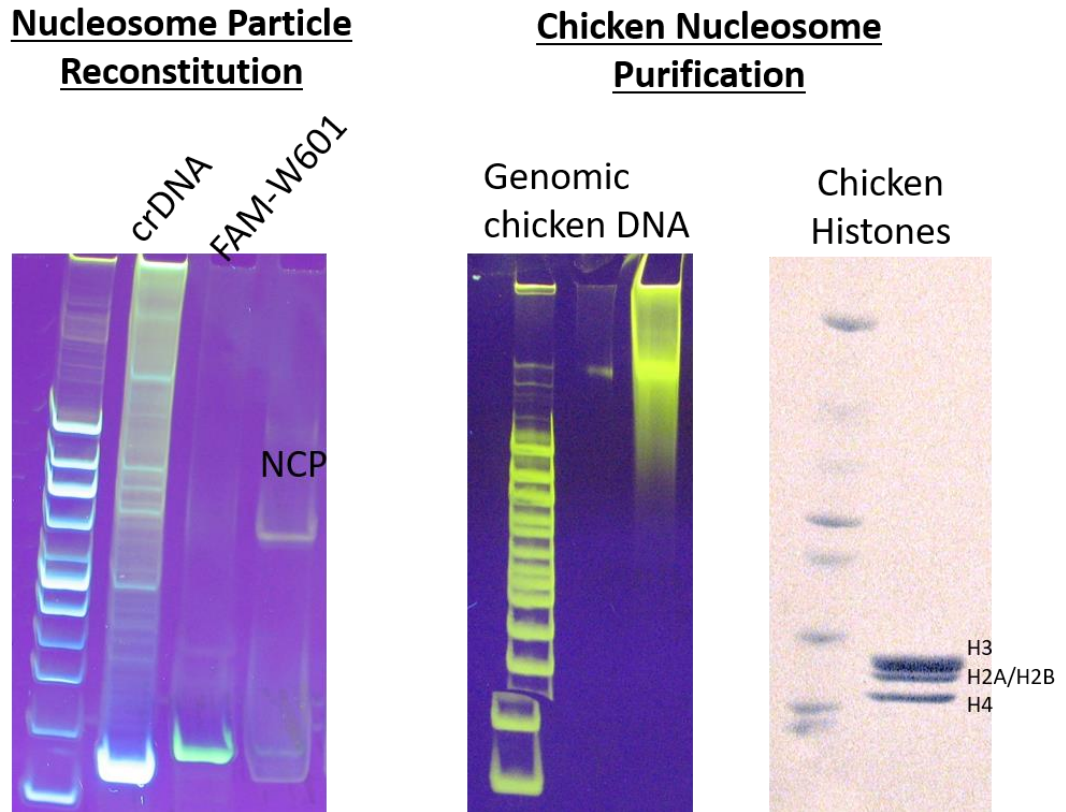


Figure 14: Nucleosomal DNA preparation. Left panel: Native TBE polyacrylamide gel demonstrating confirmation of crDNA, FAM labeled W601 DNA, and reconstitution of nucleosome core particle. Right panel: Native TBE polyacrylamide gel demonstrating presence of genomic chicken DNA after purification from chicken blood. SDS-PAGE demonstrating presence of histone octamer after purification from chicken blood.

Chapter 5: Conclusions and future perspectives

5.1 MECP2 AND CREB1

Our current work analyzes interactions between MeCP2 and CREB1, which have not been previously examined using biochemical techniques. We have taken advantage of the significant differences in isoelectric points (pI) in MeCP2 and CREB1, and used native PAGE analysis to determine complex formation. We observed a significant change in band intensity, which correlated with the predicted pI of the MeCP2/CREB1 complex. We speculate that full length MeCP2 and CREB1 are forming a complex and are migrating out of the gel. In comparison to the results from the full length MeCP2, MeCP2 MBD-ATH1 demonstrates less of a decrease in band intensity. This suggests that the TRD is probably involved in the interactions between MeCP2 and CREB1. Future work to analyze MeCP2/CREB1 complexing through gel electrophoresis would include isoelectric focusing, which separates proteins and protein complexes based on their isoelectric point. We would like to dissect more information on which domains are involved in these interactions by testing the DNA binding domain of CREB1 as well.

We also analyzed the effect of MeCP2 on CREB1 binding to its CRE target site. We first determined the affinity of MeCP2 to our probe containing the specific site for CREB binding and found that it has a low dissociation constant, which means it has a high affinity. To determine if this was due to nonspecific interactions or some type of sequence specificity, we used a different nonspecific probe of the same length, and same FAM label on the 5' terminal end. MeCP2 also exhibited a high affinity for this DNA, indicating that MeCP2 binds very tightly to nonspecific sequences. Next, we determined the binding affinity of CREB1 to its target sequence and found very low affinity binding. After determining that CREB1 is extremely sensitive to oxidation, we repeated the same experiment under reducing conditions, and found that CREB1 did display a stronger

affinity. We speculate that the initial binding assay demonstrated a weak affinity due to the presence of oxidation products. Although CREB1 did bind to this probe, the affinity is still weak in comparison to most sequence specific DNA binding proteins. This may be due to CREB1 being in an unphosphorylated state. *In vivo*, CREB1 transcriptional activity is activated through phosphorylation at Ser133.⁶³ Future work requires *in vitro* site specific phosphorylation to determine if the affinity is affected by the lack of phosphorylation. Another possibility is that CREB1 may not be properly or completely refolded. This is unlikely since it only has one structured region, which is the DNA binding domain that consists of a single alpha helix. CREB1 is a homodimeric protein, so there is also a possibility it did not dimerize completely. In the future, we plan to express the protein and label isotopically to conduct NMR experiments and examine folding state by comparing to NMR signals in literature. Finally, we conducted binding assays of CREB1 to its target site in the presence of MeCP2 and observed interesting results, where the presence of MeCP2 at a relatively high concentration seemed to impede CREB1 binding to its target, while a much lower concentration didn't affect binding. These assays require optimization, where the concentration of MeCP2 is adjusted to bypass the strong binding effect to nonspecific DNA, in order to observe CREB1 binding. Protein-protein interactions also typically cause an enthalpic change. We plan to conduct isothermal calorimetry assays to determine if there is an enthalpy change when MeCP2 is titrated to a solution of CREB1. Finally, we would like to conduct the same binding studies using the MeCP2 MBD-ATH1 construct, to determine effects of removing the TRD, and CREB1 bZIP DNA binding domain. This would allow us to gain a general understanding of what domains are implicated in MeCP2/CREB1 interactions.

CREB1 and MeCP2 have both been shown to be critical regulators in the brain. In addition both CREB1 and MeCP2 levels are affected. Cocaine usage has been demonstrated to increase transcription of the CREB1 gene target, brain derived neurotrophic factor (BDNF). Cocaine induces MeCP2 phosphorylation which causes it to

dissociate from the methylated BDNF promoter, while simultaneously increasing phosphorylation of CREB1 that causes association to the BDNF promoter.⁶⁴ CREB1 and MeCP2 have been reported to compete for the BDNF promoter to reveal a complicated network that is present in cocaine addicted neurons.⁶⁵ Studying potential MeCP2/CREB1 interactions are important to further dissect details of this network in the brain during cocaine action.

5.2 NUCLEOSOMAL DNA IN TARGET SEARCH

We have made significant progress to study how factors like DNA methylation and natural decoys in the genome affect transcription factor target search. We tested how these factors affect target search, and the results supported our hypothetical model of MeCP2 indirectly activating transcription. We also want to study how chromatin organization may affect target search. To conduct this, we needed to establish preliminary protocols in our lab to assemble nucleosome core particles. We reconstituted mononucleosomes *in vitro* through dialysis, and purified chromatin from chicken blood. The chromatin isolated from chicken blood can be further purified to obtain chicken histone octamers, which we can then use to reconstitute nucleosomes. In the future, we plan to establish a protocol that produces a high, pure yield of nucleosomes in order to analyze biophysically, and to study the effect on transcription factor target search.

Bibliography

1. Alberts, B.; Johnson, A.; Lewis, J.; Morgan, D.; Raff, M.; Roberts, K.; Walter, P., *Molecular Biology of the Cell, Sixth Edition*. Taylor & Francis Group: 2014.
2. Thurman, R. E.; Rynes, E.; Humbert, R.; Vierstra, J.; Maurano, M. T.; Haugen, E.; Sheffield, N. C.; Stergachis, A. B.; Wang, H.; Vernot, B., The accessible chromatin landscape of the human genome. *Nature* **2012**, *489* (7414), 75.
3. Yang, L.; Orenstein, Y.; Jolma, A.; Yin, Y.; Taipale, J.; Shamir, R.; Rohs, R., Transcription factor family-specific DNA shape readout revealed by quantitative specificity models. *Molecular systems biology* **2017**, *13* (2), 910.
4. Badis, G.; Berger, M. F.; Philippakis, A. A.; Talukder, S.; Gehrke, A. R.; Jaeger, S. A.; Chan, E. T.; Metzler, G.; Vedenko, A.; Chen, X., Diversity and complexity in DNA recognition by transcription factors. *Science* **2009**, *324* (5935), 1720-1723.
5. Klug, A.; Schwabe, J., Protein motifs 5. Zinc fingers. *The FASEB journal* **1995**, *9* (8), 597-604.
6. Cao, X.; Koski, R.; Gashler, A.; McKiernan, M.; Morris, C.; Gaffney, R.; Hay, R.; Sukhatme, V., Identification and characterization of the Egr-1 gene product, a DNA-binding zinc finger protein induced by differentiation and growth signals. *Molecular and cellular biology* **1990**, *10* (5), 1931-1939.

7. Syed, K. S.; He, X.; Tillo, D.; Wang, J.; Durell, S. R.; Vinson, C., 5-Methylcytosine (5mC) and 5-Hydroxymethylcytosine (5hmC) Enhance the DNA Binding of CREB1 to the C/EBP Half-Site Tetranucleotide GCAA. *Biochemistry* **2016**, *55* (49), 6940-6948.
8. Benbrook, D. M.; Jones, N. C., Different binding specificities and transactivation of variant CRE's by CREB complexes. *Nucleic Acids Research* **1994**, *22* (8), 1463-1469.
9. Lonze, B. E.; Ginty, D. D., Function and regulation of CREB family transcription factors in the nervous system. *Neuron* **2002**, *35* (4), 605-623.
10. Herdegen, T.; Leah, J. D., Inducible and constitutive transcription factors in the mammalian nervous system: control of gene expression by Jun, Fos and Krox, and CREB/ATF proteins. *Brain Research Reviews* **1998**, *28* (3), 370-490.
11. Winter, R. B.; Berg, O. G.; Von Hippel, P. H., Diffusion-driven mechanisms of protein translocation on nucleic acids. 3. The Escherichia coli lac repressor-operator interaction: kinetic measurements and conclusions. *Biochemistry* **1981**, *20* (24), 6961-6977.
12. Berg, O. G.; Winter, R. B.; Von Hippel, P. H., Diffusion-driven mechanisms of protein translocation on nucleic acids. 1. Models and theory. *Biochemistry* **1981**, *20* (24), 6929-6948.
13. Schmidt, H. G.; Sewitz, S.; Andrews, S. S.; Lipkow, K., An Integrated Model of Transcription Factor Diffusion Shows the Importance of Intersegmental Transfer and Quaternary Protein Structure for Target Site Finding. *PloS one* **2014**, *9* (10), e108575.

14. Kemme, C. A.; Nguyen, D.; Chattopadhyay, A.; Iwahara, J., Regulation of transcription factors via natural decoys in genomic DNA. *Transcription* **2016**, *7* (4), 115-120.
15. Kemme, C. A.; Esadze, A.; Iwahara, J., Influence of quasi-specific sites on kinetics of target DNA search by a sequence-specific DNA-binding protein. *Biochemistry* **2015**, *54* (44), 6684-6691.
16. Weber, M.; Hellmann, I.; Stadler, M. B.; Ramos, L.; Pääbo, S.; Rebhan, M.; Schübeler, D., Distribution, silencing potential and evolutionary impact of promoter DNA methylation in the human genome. *Nature genetics* **2007**, *39* (4), 457.
17. Bird, A. P., CpG-rich islands and the function of DNA methylation. *Nature* **1986**, *321* (6067), 209-213.
18. Skene, P. J.; Illingworth, R. S.; Webb, S.; Kerr, A. R. W.; James, K. D.; Turner, D. J.; Andrews, R.; Bird, A. P., Neuronal MeCP2 Is Expressed at Near Histone-Octamer Levels and Globally Alters the Chromatin State. *Molecular cell* **2010**, *37* (4), 457-468.
19. Jones, P. A.; Takai, D., The role of DNA methylation in mammalian epigenetics. *Science* **2001**, *293* (5532), 1068-1070.
20. Ramirez-Carrozzi, V. R.; Braas, D.; Bhatt, D. M.; Cheng, C. S.; Hong, C.; Doty, K. R.; Black, J. C.; Hoffmann, A.; Carey, M.; Smale, S. T., A unifying model for the selective regulation of inducible transcription by CpG islands and nucleosome remodeling. *Cell* **2009**, *138* (1), 114-128.

21. Saxonov, S.; Berg, P.; Brutlag, D. L., A genome-wide analysis of CpG dinucleotides in the human genome distinguishes two distinct classes of promoters. *Proceedings of the National Academy of Sciences* **2006**, *103* (5), 1412-1417.
22. Jones, P. A., Functions of DNA methylation: islands, start sites, gene bodies and beyond. *Nature reviews. Genetics* **2012**, *13* (7), 484.
23. Fatemi, M.; Wade, P. A., MBD family proteins: reading the epigenetic code. *Journal of cell science* **2006**, *119* (15), 3033-3037.
24. Lubin, F. D.; Roth, T. L.; Sweatt, J. D., Epigenetic regulation of BDNF gene transcription in the consolidation of fear memory. *Journal of Neuroscience* **2008**, *28* (42), 10576-10586.
25. Yang, Y.; Kucukkal, T. G.; Li, J.; Alexov, E.; Cao, W., Binding analysis of methyl-CpG binding domain of MeCP2 and Rett syndrome mutations. *ACS chemical biology* **2016**, *11* (10), 2706-2715.
26. (a) Kumar, A.; Kamboj, S.; Malone, B. M.; Kudo, S.; Twiss, J. L.; Czymmek, K. J.; LaSalle, J. M.; Schanen, N. C., Analysis of protein domains and Rett syndrome mutations indicate that multiple regions influence chromatin-binding dynamics of the chromatin-associated protein MECP2 in vivo. *Journal of cell science* **2008**, *121* (7), 1128-1137; (b) Baker, S. A.; Chen, L.; Wilkins, A. D.; Yu, P.; Lichtarge, O.; Zoghbi, H. Y., An AT-hook domain in MeCP2 determines the clinical course of Rett syndrome and related disorders. *Cell* **2013**, *152* (5), 984-996.
27. Wakefield, R. I. D.; Smith, B. O.; Nan, X.; Free, A.; Soteriou, A.; Uhrin, D.; Bird, A. P.; Barlow, P. N., The solution structure of the domain from MeCP2 that binds to

- methylated DNA¹¹ Edited by P. E. Wright. *Journal of molecular biology* **1999**, 291 (5), 1055-1065.
28. Kruusvee, V.; Lyst, M. J.; Taylor, C.; Tarnauskaitė, Ž.; Bird, A. P.; Cook, A. G., Structure of the MeCP2–TBLR1 complex reveals a molecular basis for Rett syndrome and related disorders. *Proceedings of the National Academy of Sciences* **2017**, 114 (16), E3243-E3250.
29. Chia, J. Y.; Tan, W. S.; Ng, C. L.; Hu, N.-J.; Foo, H. L.; Ho, K. L., A/T run geometry of B-form DNA is independent of bound Methyl-CpG binding domain, cytosine methylation and flanking sequence. *Scientific reports* **2016**, 6.
30. Guy, J.; Cheval, H.; Selfridge, J.; Bird, A., The role of MeCP2 in the brain. *Annual review of cell and developmental biology* **2011**, 27, 631-652.
31. Lyst, M. J.; Bird, A., Rett syndrome: a complex disorder with simple roots. *Nature Reviews Genetics* **2015**, 16, 261.
32. Nan, X.; Ng, H.-H.; Johnson, C. A.; Laherty, C. D.; Turner, B. M.; Eisenman, R. N.; Bird, A., Transcriptional repression by the methyl-CpG-binding protein MeCP2 involves a histone deacetylase complex. *Nature* **1998**, 393 (6683), 386.
33. Georgel, P. T.; Horowitz-Scherer, R. A.; Adkins, N.; Woodcock, C. L.; Wade, P. A.; Hansen, J. C., Chromatin compaction by human MeCP2 assembly of novel secondary chromatin structures in the absence of DNA methylation. *Journal of Biological Chemistry* **2003**, 278 (34), 32181-32188.

34. Chahrour, M.; Jung, S. Y.; Shaw, C.; Zhou, X.; Wong, S. T.; Qin, J.; Zoghbi, H. Y., MeCP2, a key contributor to neurological disease, activates and represses transcription. *Science* **2008**, *320* (5880), 1224-1229.
35. Yasui, D. H.; Peddada, S.; Bieda, M. C.; Vallero, R. O.; Hogart, A.; Nagarajan, R. P.; Thatcher, K. N.; Farnham, P. J.; LaSalle, J. M., Integrated epigenomic analyses of neuronal MeCP2 reveal a role for long-range interaction with active genes. *Proceedings of the National Academy of Sciences* **2007**, *104* (49), 19416-19421.
36. Kemme, C. A.; Marquez, R.; Luu, R. H.; Iwahara, J., Potential role of DNA methylation as a facilitator of target search processes for transcription factors through interplay with methyl-CpG-binding proteins. *Nucleic Acids Research* **2017**.
37. Suzuki, M. M.; Kerr, A. R.; De Sousa, D.; Bird, A., CpG methylation is targeted to transcription units in an invertebrate genome. *Genome research* **2007**, *17* (5), 625-631.
38. Shen, L.; Kondo, Y.; Guo, Y.; Zhang, J.; Zhang, L.; Ahmed, S.; Shu, J.; Chen, X.; Waterland, R. A.; Issa, J.-P. J., Genome-wide profiling of DNA methylation reveals a class of normally methylated CpG island promoters. *PLoS genetics* **2007**, *3* (10), e181.
39. Esadze, A.; Iwahara, J., Stopped-flow fluorescence kinetic study of protein sliding and intersegment transfer in the target DNA search process. *Journal of molecular biology* **2014**, *426* (1), 230-244.
40. Zandarashvili, L.; White, M. A.; Esadze, A.; Iwahara, J., Structural impact of complete CpG methylation within target DNA on specific complex formation of the inducible transcription factor Egr-1. *FEBS Letters* **2015**, *589* (15), 1748-1753.

41. Leonard, H.; Bower, C.; English, D., The prevalence and incidence of Rett syndrome in Australia. *European child & adolescent psychiatry* **1997**, *6*, 8-10.
42. Meloni, I.; Bruttini, M.; Longo, I.; Mari, F.; Rizzolio, F.; D'Adamo, P.; Denvriendt, K.; Fryns, J.-P.; Toniolo, D.; Renieri, A., A mutation in the Rett syndrome gene, MECP2, causes X-linked mental retardation and progressive spasticity in males. *The American Journal of Human Genetics* **2000**, *67* (4), 982-985.
43. Webb, T.; Latif, F., Rett syndrome and the MECP2 gene. *Journal of medical genetics* **2001**, *38* (4), 217-223.
44. Kaufmann, W. E.; Glaze, D. G.; Christodoulou, J.; Clarke, A. J.; Bahi-Buisson, N.; Leonard, H.; Bailey, M. E.; Schanen, N. C.; Zappella, M.; Renieri, A., Rett syndrome: revised diagnostic criteria and nomenclature. *Annals of neurology* **2010**, *68* (6), 944-950.
45. Moretti, P.; Zoghbi, H. Y., MeCP2 dysfunction in Rett syndrome and related disorders. *Current opinion in genetics & development* **2006**, *16* (3), 276-281.
46. Yazdani, M.; Deogracias, R.; Guy, J.; Poot, R. A.; Bird, A.; Barde, Y. A., Disease modeling using embryonic stem cells: MeCP2 regulates nuclear size and RNA synthesis in neurons. *Stem cells* **2012**, *30* (10), 2128-2139.
47. Chahrour, M.; Zoghbi, H. Y., The story of Rett syndrome: from clinic to neurobiology. *Neuron* **2007**, *56* (3), 422-437.
48. Cheng, T.-L.; Qiu, Z., MeCP2: multifaceted roles in gene regulation and neural development. *Neuroscience bulletin* **2014**, *30* (4), 601-609.
49. Krishnaraj, R.; Ho, G.; Christodoulou, J., RettBASE: Rett Syndrome Database Update. *Human Mutation* **2017**.

50. Amir, R. E.; Van den Veyver, I. B.; Wan, M.; Tran, C. Q.; Francke, U.; Zoghbi, H. Y., Rett syndrome is caused by mutations in X-linked MECP2, encoding methyl-CpG-binding protein 2. *Nature genetics* **1999**, *23* (2), 185-188.
51. Massart, R.; Freyburger, M.; Suderman, M.; Paquet, J.; El Helou, J.; Belanger-Nelson, E.; Rachalski, A.; Koumar, O.-C.; Carrier, J.; Szyf, M., The genome-wide landscape of DNA methylation and hydroxymethylation in response to sleep deprivation impacts on synaptic plasticity genes. *Translational psychiatry* **2014**, *4* (1), e347.
52. Lim, U.; Song, M.-A., Dietary and lifestyle factors of DNA methylation. *Cancer epigenetics: methods and protocols* **2012**, 359-376.
53. Banik, A.; Kandilya, D.; Ramya, S.; Stünkel, W.; Chong, Y. S.; Dheen, S. T., Maternal Factors that Induce Epigenetic Changes Contribute to Neurological Disorders in Offspring. *Genes* **2017**, *8* (6), 150.
54. Ma, D. K.; Marchetto, M. C.; Guo, J. U.; Ming, G.-l.; Gage, F. H.; Song, H., Epigenetic choreographers of neurogenesis in the adult mammalian brain. *Nature neuroscience* **2010**, *13* (11), 1338-1344.
55. Torres, R. F.; Hidalgo, C.; Kerr, B., Mecp2 Mediates Experience-Dependent Transcriptional Upregulation of Ryanodine Receptor Type-3. *Frontiers in Molecular Neuroscience* **2017**, *10* (188).
56. Guo, J. U.; Ma, D. K.; Mo, H.; Ball, M. P.; Jang, M.-H.; Bonaguidi, M. A.; Balazer, J. A.; Eaves, H. L.; Xie, B.; Ford, E., Neuronal activity modifies the DNA methylation landscape in the adult brain. *Nature neuroscience* **2011**, *14* (10), 1345-1351.

57. Lavallie, E. R.; DiBlasio, E. A.; Kovacic, S.; Grant, K. L.; Schendel, P. F.; McCoy, J. M., A thioredoxin gene fusion expression system that circumvents inclusion body formation in the E. coli cytoplasm. *Nature biotechnology* **1993**, *11* (2), 187.
58. Gasparian, M. E.; Ostapchenko, V. G.; Yagolovich, A. V.; Tsygannik, I. N.; Chernyak, B. V.; Dolgikh, D. A.; Kirpichnikov, M. P., Overexpression and refolding of thioredoxin/TRAIL fusion from inclusion bodies and further purification of TRAIL after cleavage by enteropeptidase. *Biotechnology letters* **2007**, *29* (10), 1567-1573.
59. Fiala, G. J.; Schamel, W. W. A.; Blumenthal, B., Blue Native Polyacrylamide Gel Electrophoresis (BN-PAGE) for Analysis of Multiprotein Complexes from Cellular Lysates. *Journal of Visualized Experiments : JoVE* **2011**, (48), 2164.
60. Nikitina, T.; Shi, X.; Ghosh, R. P.; Horowitz-Scherer, R. A.; Hansen, J. C.; Woodcock, C. L., Multiple modes of interaction between the methylated DNA binding protein MeCP2 and chromatin. *Molecular and cellular biology* **2007**, *27* (3), 864-877.
61. Bilokapic, S.; Strauss, M.; Halic, M., Histone octamer rearranges to adapt to DNA unwrapping. *Nature structural & molecular biology* **2018**, *25* (1), 101-108.
62. Lowary, P. T.; Widom, J., New DNA sequence rules for high affinity binding to histone octamer and sequence-directed nucleosome positioning | Edited by T. Richmond. *Journal of molecular biology* **1998**, *276* (1), 19-42.
63. Mayr, B.; Montminy, M., Transcriptional regulation by the phosphorylation-dependent factor CREB. *Nature Reviews Molecular Cell Biology* **2001**, *2*, 599.
64. McCarthy, D. M.; Brown, A. N.; Bhide, P. G., Regulation of BDNF Expression by Cocaine. *The Yale Journal of Biology and Medicine* **2012**, *85* (4), 437-446.

65. Feng, J.; Nestler, E. J., MeCP2 and drug addiction. *Nature neuroscience* **2010**, *13* (9), 1039.

Vita

Esmeralda Martinez was born on November 11th, 1994, to Adrian and Maria Martinez in Houston, Texas. Esmeralda received a Bachelor of Science in Chemistry with a concentration in biochemistry and minor in biology from the University of Houston-Downtown in Houston, Texas. She graduated in May 2016 with Magna Cum Laude institutional honors. She entered the Biochemistry and Molecular Biology graduate program at the University of Texas Medical Branch (UTMB) in August 2016. She joined Dr. Junji Iwahara's lab in the Biochemistry and Molecular Biology department to work on studying protein/DNA interactions. At UTMB, she has received the Arthur V. Simmang Graduate School of Biomedical Sciences Scholarship and has participated as a mentor in the Biomedical Research Training Program for High School Students Program. She has also served as the Co-Chair for the Biochemistry Journal Club, and Secretary for the Biological Chemistry Student Organization.

Permanent address: 9715 Coahuila St.
Houston, Texas 77013.

This thesis was typed by Esmeralda Martinez.